



Effect of Aromatic Rings in AESO-VDM Biopolymers on the Local Free Volume and Diffusion Properties of Polymer Matrix

David Pavel Královič¹ · Katarína Cifraničová¹ · Helena Švajdlenková^{1,2} · Darina Tóthová¹ · Ondrej Šauša^{1,3} · Pavol Kalinay³ · Taras Kavetsky^{3,4} · Jolita Ostrauskaite⁵ · Oleh Smutok⁶ · Mykhailo Gonchar⁷ · Vladimir Soloviev⁸ · Arnold Kiv^{9,10}

Accepted: 17 October 2023
© The Author(s) 2023

Abstract

In this work, the influence of aromatic rings on the local free volume of cured mixtures of acrylate epoxidized soybean oil (AESO) and vanillin dimethacrylate (VDM) was investigated. Cross-linking took place under the influence of UV light in the presence or absence of a photoinitiator. The local free volume and its homogeneity were characterized using the Positron Annihilation Lifetime Spectroscopy (PALS) technique. It was found that increasing the content of VDM, which contains aromatic rings, caused a decrease in the local free volume of the cured polymer network, with consequences for the diffusion properties of the polymer, which were tested for the case of water. Another consequence of increasing the content of VDM was a decrease in the conversion of double bonds in the finally cured samples, characterized by near-infrared spectroscopy (NIR). This finding illustrates a case where the decrease in free volume is not necessarily related to an increase in the crosslinking density of the polymer, but is a consequence of the presence of an increase in the occupied volume of aromatic rings in the volume of the polymer.

Keywords Biopolymers · Photopolymerization · Crosslinking · Positron annihilation lifetime spectroscopy · Free volume · Diffusion properties

Introduction

Photopolymerization is a process that changes the structure of monomers and oligomers after exposure to light, often in the ultraviolet or visible region of the electromagnetic spectrum. These changes are manifested structurally, most often by hardening of the material due to cross-linking. The

advantages of this process are low energy consumption, high efficiency, low level of produced emissions of volatile organic compounds and a large number of applications not only in common areas such as coatings, inks and adhesives, but also in high-tech domains, such as microelectronics, optoelectronics, laser imaging, stereolithography and nanotechnology [1–4].

✉ Helena Švajdlenková
helena.svajdlenkova@savba.sk

✉ Taras Kavetsky
kavetsky@yahoo.com

¹ Department of Nuclear Chemistry, Comenius University in Bratislava, 842 15 Bratislava, Slovakia

² Polymer Institute, Slovak Academy of Sciences, 845 41 Bratislava, Slovakia

³ Institute of Physics, Slovak Academy of Sciences, 845 11 Bratislava, Slovakia

⁴ Department of Biology and Chemistry, Drohobych Ivan Franko State Pedagogical University, 82100 Drohobych, Ukraine

⁵ Department of Polymer Chemistry and Technology, Kaunas University of Technology, 50254 Kaunas, Lithuania

⁶ Department of Chemistry and Biomolecular Science, Clarkson University, 13699 Potsdam, NY, USA

⁷ Institute of Cell Biology, National Academy of Sciences of Ukraine, 79005 Lviv, Ukraine

⁸ Kryvyi Rih State Pedagogical University, 50086 Kryvyi Rih, Ukraine

⁹ Department of Innovation Technologies, South-Ukrainian K.D. Ushynsky National Pedagogical University, 65020 Odesa, Ukraine

¹⁰ Department of Materials Engineering, Ben-Gurion University of the Negev, 84105 Beer-Sheva, Israel

The application of photopolymers as adhesion matrices for enzymes immobilization is the subject of current research in biosensor systems, as it has been shown that enzyme immobilization to the surface of polymer and its sensitivity and selectivity are influenced by the microstructure of the polymer [5]. This type of matrix was also studied from the point of view of the local free volume in some recent works, but it was a mutual comparison of the properties for hardened samples of a different composition [6, 7]. Changes in the intermolecular space of acrylate epoxidized soybean oil (AESO)-based samples during photopolymerization, as well as the characterization of the free volume properties of the final network from the point of view of the amount of added vanillin dimethacrylate (VDM) with aromatic rings and presence of photoinitiator, which affect the local free volume, have not been studied so far. Only a study was carried out that related to the characterization of the properties of the final AESO-VDM copolymer network with molar ratios of 1:0.5 from the point of view of the correlation of local free volumes with the operating parameters of highly sensitive biosensors [8]. Thus, a more detailed analysis of the effect of the amount of comonomer with aromatic rings is missing, which affects the local free volume between the chains of the network, which results in a change in the diffusion properties of the polymer network. At the same time, the work [8] shows that AESO-VDM copolymers (without the addition of a photoinitiator) have the most favorable amperometric properties of the studied materials used as an immobilization matrix for the construction of biosensors. For their potential use in bioelectrodes, a more detailed study of these materials from different perspectives is therefore interesting.

Local free volume and its changes in solids can be studied by a variety of standard techniques that are applicable at different dimensional scales or degrees of order. Positron annihilation lifetime spectroscopy (PALS) is one of the sensitive techniques for the investigation of cavity dimensions in the 0.1–50 nm scale and thus also for investigating the microstructure [9, 10]. The technique is based on the measurement of positron or positronium (the bound state of an electron with a positron, Ps) lifetimes. The triplet state of the positronium, the ortho-positronium (*o*-Ps), is crucial for determining the size of local free volumes. Using this technique, it is possible to characterize not only the final polymer network after curing via its free-volume properties [11], but also the course of the local free volume during the cross-linking process, which accompanies the course of photopolymerization [12].

A certain problem in determining the real size of the local free volume in the liquid phase using the PALS technique is the so-called “bubble effect” [13–15]. In this case, the positronium probe creates its own cavity, a bubble, by its movement, and then the lifetime of the probe overestimates

the real dimensions of the intermolecular spaces. However, in the case of time dependence of *o*-Ps lifetimes observed in the liquid phase of the investigated samples, when relative lifetime changes are involved, it is not necessary to consider the contribution of the bubble effect in the monomers.

Our goal was to investigate the microstructural characteristics of potentially suitable photopolymers, based on natural oils, as enzyme adhesion matrices in biosensor systems with an emphasis on information on local free-volume during the course of sample crosslinking, and final cross-linked polymers as a consequence of the chemical composition. We mean the influence of the photoinitiator and the amount of VDM comonomer with aromatic rings responsible for stacking π – π interactions that affect the network structure and the local free volume.

Briefly, in other words, the aim of the work is to investigate how the number of aromatic rings of the VDM comonomer in AESO and the presence of a photoinitiator influence the course of the photopolymerization reaction and the final properties of the network from a free volume point of view.

Experimental

Examined Samples

The input materials used for photopolymerization were sets of 8 viscous solutions containing acrylated epoxidized soybean oil (AESO) and vanillin dimethacrylate (VDM) with molar ratio of monomers: AESO:VDM 1:0, 1:0.25, 1:0.5, 1:1, and with or without the addition of a photoinitiator (PI), i.e. 2,2-dimethoxy-2-phenylacetophenone (DMPA). 3 mol% of PI, calculated from the total molar amount of all monomers, was used. AESO and DMPA were purchased from Sigma-Aldrich. VDM was purchased from Specific Polymers. The addition of VDM into the AESO leads to a higher viscosity of the mixture [16–20]. The chemical structure of the used monomers and PI is shown in Table 1.

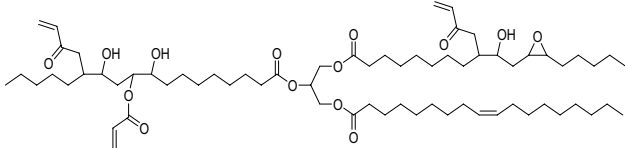
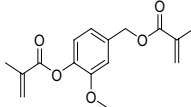
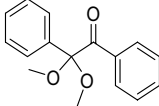
Illumination of Samples

A Jaxman U1 LED light source in the UV region at 365 nm was used to photopolymerize a series of AESO/VDM samples. To ensure constant light intensity over time an adjusted LED power supply through an E36106A stabilized current source (Keysight Technologies) was used. The light intensity was measured and adjusted using an Ophir Photonics StarLite meter with a PD300-UV probe.

PALS

For the purposes of PALS measurements, a silicone chamber was made for the sample with an inner diameter of

Table 1 Chemical structure of used monomers and photoinitiator [16]

Materials	Chemical structure
Acrylated epoxidized soybean oil (AESO)	
Vanillin dimethacrylate (VDM)	
2,2-dimethoxy-2-phenylacetophenone (photoinitiator; PI)	

15 mm and a height of 3 mm corresponding to the geometry of the sample. The bottom part of PALS chamber contained a quartz glass window for UV light and the upper part was covered by a protective film from Kapton. In our experiments, a “sample-positron source-reference sample” sandwich arrangement was used. Such an arrangement of the investigated sample from only one side of the positron source was chosen due to the precise definition of the light intensity in the sample, which was illuminated from one side. Thus eliminating the possibility of interference of possible small differences of synthesis in two different independent volumes was eliminated. A more detailed view of the mentioned arrangement is in Figure S1 in the SI.

Defect-free aluminium was used as a reference in a sandwich arrangement. The PALS spectrometer consisted of two scintillation detectors 25.4B12/2 M-Q-BAF-X-N (Scionix, The Netherlands), a digital acquisition system based on the DRS4 V5 digitizer (PSI, Switzerland) and Q-PALS software [21, 22].

The chamber for the sample together with the positron source and the Al reference sample was placed between the detectors. It was measured at a room temperature of 20 °C. The source of positrons was radioactive sodium ^{22}Na with an activity of approx. 2 MBq. The time resolution of the spectrometer was approx. 330 ps (full width at half maximum of resolution curve). The time resolution function of the spectrometer was determined using defect-free Al. The annihilation in the positron source and Kapton foils was also included in the analyses of the time spectra.

Lifetime spectra consist of several components with different average lifetimes, which are associated with different processes of annihilation, both direct and annihilation

of the bound state of an electron and a positron, the so-called positronium, Ps. The bound state of Ps can be in the ortho and para states (*o*-Ps and *p*-Ps, respectively) which differ in their spin and lifetime. Generally, the measured lifetime spectra for polymers, the shortest lifetime is associated with *p*-Ps annihilation, a longer component with annihilation in the bulk, smaller cavities and defects of the polymer chain, and a long lifetime is associated with pick-off annihilation of *o*-Ps in large cavities. In materials such as polymers, an orthopositronium localized in a pore interacts with an electron from the wall of cavity such that the electron annihilates with the positron from *o*-Ps by a two-photon annihilation process (“pick-off” annihilation) with shortened lifetime, compared to vacuum value (142 ns). This shortened orthopositronium lifetime is proportional to the pore size.

The measured lifetime spectra were analyzed using the LT program [23], LT Polymers™ version. In our case, spectra consisting of four components, but only the longest one, associated with the pick-off process of *o*-Ps annihilation, were investigated in more detail. The shorter components were related to the direct annihilation in the Al reference (fixed at 166 ps) and to the annihilation of *p*-Ps (fixed at 125 ps) in the polymer. The ratio of the intensities of the *o*-Ps and *p*-Ps components was fixed at 3:1. LT program allows the evaluation of lifetime spectra in discrete or continuous mode.

A frequently used correlation between the lifetime of *ortho*-positronium and the size of free volumes is the semi-empirical quantum-mechanical Tao-Eldrup model [24, 25], based on which the radii of spherical local free volumes and the volume of free volume holes are determined.

The idea of spherical cavities in polymers is a considerable simplification of the real situation, but it is sufficient for a relative comparison of the samples. The relationship (1) follows from the Tao-Eldrup model:

$$\tau_{o-Ps} = 0.5 \left\{ 1 - \frac{R}{R + \Delta R} + \frac{1}{2\pi} \sin \left[\frac{2\pi R}{R + \Delta R} \right] \right\}^{-1} \quad (1)$$

where τ_{o-Ps} represents the ortho-positronium lifetime in nanoseconds, R is the radius of the spherical cavity in nm and ΔR is a parameter interpreted as the thickness of the electron layer and at the same time as an empirical constant, determined from annihilation measurements of various porous substances. Its value is 0.166 nm. The size of the spherical cavity is calculated as follows:

$$V_h = \frac{4}{3} \pi R^3 \quad (2)$$

Swelling

Material samples were weighed on a VWR Semimicro balance SMG 425i laboratory balance (with a maximum weight of 42 g and the smallest fraction of 0.01 mg) and then placed in water (CHROMASOLV™, type LC-MS Ultra from Honeywell/Riedel-de Haen) with relative molecular weight $M_r = 18.0153 \text{ g mol}^{-1}$ and closed (20 °C). After approximately six hours, the samples were removed from the water, dried with a paper towel and then weighed again. After weighing, the samples were again immersed in water. This procedure was repeated several times until the samples reached the saturated state.

NIR Spectroscopy

The series of the samples without and with PI was measured in a fiber-coupled cuvette holder BW Tek with two optical-fiber cables of diameter 100 μm connected to BW Tek detector (Sol. 2.2) and light source BPS 2.0 with the spectral range (350–2600 nm). The spectra were registered in the wavenumber range 4500–9200 cm^{-1} .

Thermocouple Temperature Measurements

Temperature measurements during photopolymerization were carried out using a measurement system developed at the Institute of Physics of the SAS [26]. T-type thermocouples (Omega Engineering) record the temperature every 1 s. The temperature-measuring thermocouple had a measuring tip 4 mm away from the inner edge of the silicon chamber used in PALS measurement and at half the height of the sample space. Such prepared PALS chamber was placed above the UV light source identically to the PALS measurement.

Results and Discussion

The effect of aromatic rings on the free volume properties and the consequences on the diffusion properties of the polymer network has been studied from several perspectives. First, the time evolution of crosslinking as a function of the amount of VDM was monitored using temperature and free-volume changes. In the second step, the free-volume properties of the cured biopolymers were characterized using the PALS technique and the results were confronted with the degree of crosslinking using NIR spectroscopy. In the last step, the consequences of the bulk properties of networks with different VDM contents on their diffusion properties for water were studied.

In Situ Polymerization Monitoring by Thermocouple (TC)

The in situ temperature measurement of the continuously irradiated AESO and AESO/VDM-based samples without or with PI provides information about the kinetics. These experiments were carried out in PALS chamber with a fixed thermocouple (TC) in the middle of the reaction system and UV light from the bottom side (Fig. S1 in SI). Due to two reaction systems with or without PI, two different flux densities of 0.7 and 22.2 mW cm^{-2} of UV light were used, respectively, to achieve a similar temperature response.

In the case of the temperature response via TC, the released reaction heat is influenced by the absorption of light during irradiation and cooler aluminium edges of the sample chamber. Therefore, the absolute value of the released reaction heat is not so easy to determine. However, apart from these contributions, the time dependence of the temperature response is a very sensitive approach to study the progress of the photopolymerization (Fig. 1).

The course of the photopolymerization consists of the start of the reaction after switching on the light (waiting time until triggering of reaction), the acceleration of the reaction to the maximum polymerization rate (R_{max}) followed by a decrease in the reaction rate the so-called auto-deceleration. In addition, it is important to take into account the photoinitiated self-catalytic process of acrylates studied by Jagtap and More [27]. The saturated state with constant temperature of the cured sample at the end of illumination was obvious for AESO-based samples without PI (Fig. 1b). Moreover, in this case of samples without PI, with higher light intensity used in curing, the effect of the influence of UV light absorption by phenyl groups (present in the VDM component of the copolymer) was observed. The saturation temperature of the cured

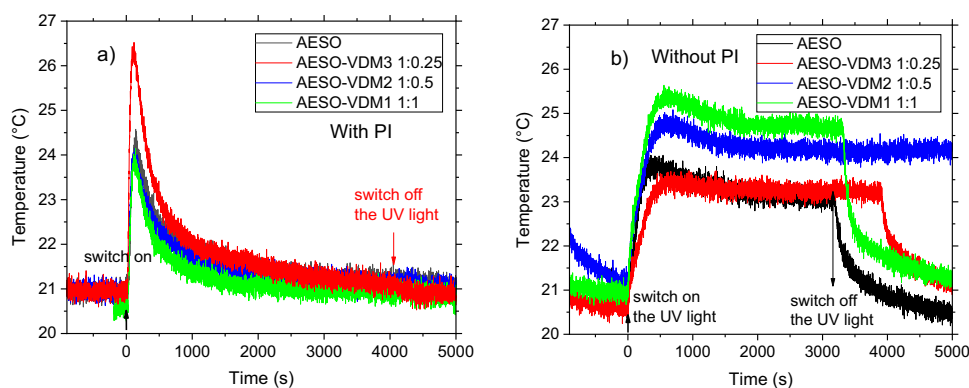


Fig. 1 Time dependence of temperature response of TC for a series of AESO-based samples with PI (a) and without PI (b). The UV light was switched on at the time of 0 s. The second arrow shows the time of switching off the UV light (for one sample only, for clarity). How-

state increased with increasing VDM concentration due to increased absorption of UV light. Finally, after switching off the UV light, the final cured sample was thermalized to room temperature.

The acceleration and deceleration time of a reaction was characterized by the rate of the temperature change (dT/dt) in Fig. S2 of SI. The times at inflection point and the maximum of the time dependence of sample temperature during photopolymerization corresponding to the maximum and the zero crossing of the 1st derivative of the (dT/dt) are given in Table 2.

Recently, the in situ study of the AESO and the comparable composition of AESO-VDM-based samples without PI by real-time photorheometry showed that AESO exhibits faster reaction compared to the samples containing VDM [16] which is in agreement with our finding t_{max} (Table 2).

In Table 2, the faster reaction of AESO with addition of VDM at the beginning (t_{IP}) than pure AESO sample implies that VDM with high absorption of UV light and faster diffusion of VDM than AESO increases its partial

reactivity in the mixture AESO-VMD. In addition, different reactivity of acrylate and methacrylate groups can also take part in the photocrosslinking and formation local structural inhomogeneities.

In the case of t_{max} , AESO-VDM samples with or without PI confirmed that an increasing amount of VDM slowing down the reaction reflecting via increasing t_{max} . This finding was also found in the study of AESO-VDM samples without PI by Lebedevaite et al. [16]. It can also be concluded that despite the lower light intensity, a series of samples with PI has a higher reactivity due to the presence of PI and increasing concentration of VDM leads to slowing down of reaction (t_{max}).

In Situ Photopolymerization Monitoring by PALS

Due to the specificity of the PALS technique, which does not allow the in-situ examination of fast processes lasting seconds or minutes directly, the course of crosslinking was investigated during intermittent illumination of the samples

Table 2 Characteristic time at the inflection point t_{IP} and the maximum t_{max} of the steep increase of the reaction corresponding to the maximum and the zero crossing of 1st derivate of the time dependence of temperature (dT/dt)

with PI	AESO	AESO-VDM3 1:0.25	AESO-VDM2 1:0.5	AESO-VDM1 1:1
t_{IP} [s]	58	37	48	49
t_{max} [s]	144	108	112	118
without PI	AESO	AESO-VDM3 1:0.25	AESO-VDM2 1:0.5	AESO-VDM1 1:1
t_{IP} [s]	30	28	28	28
t_{max} [s]	400	595	620	650

in our case. During the defined exposure time, the sample was partially cross-linked, which was followed by the measurement of lifetimes corresponding to the given degree of cross-linking. This process of intermittent irradiation was repeated until the material was completely cured. The monitored progress of the photopolymerization using the PALS technique according to the above method gives mainly data on the progress of the reaction in the later slow stages. However, the main output of these experiments is the characterization of the local free volumes of the cured samples by PALS. We note that it is also possible to reconstruct the time course of short-lived processes using PALS. However, this requires a considerably longer total measurement time and large amounts of samples (monomers). Due to the larger number of samples to be investigated, we chose a more economical option with thermocouples that also capture the initial rapid stages of the reaction.

Photopolymerization was carried out directly in the PALS chamber with a quartz window and fixed ultraviolet light from the bottom part of the sample chamber with a wavelength of 365 nm (see Fig. S1 in SI).

The irradiation conditions for the samples with the photoinitiator were as follows: the flux density of the light source at the glass window was 0.7 mW/cm^2 with a periodically repeated illumination time of 1000 s. In the case of the samples without the PI, the flux density was 22.2 mW/cm^2 and the periodic illumination time was 4300 s. The course of changes in the o -Ps lifetimes

reflecting the cross-linking changes was approximated by the exponential functions (see Fig. 2 and Table 3) for quantitative mutual comparison between the courses of the reaction of individual samples.

In the case of samples with a photoinitiator, crosslinking was comparatively faster than in the samples without PI. Therefore, a lower intensity of illumination was used for the series of samples with PI. This approach allowed us to better emphasize the differences in the time courses of cross-linking of individual samples. In Fig. 2a), the dependence of o -Ps lifetimes on the total irradiation time designed as “time” (or total light energy absorbed in the sample volume designed as “light energy”) for the samples with PI displayed a fast reaction. At the beginning of illumination, the fast crosslinking, reflected by significant changes in the lifetimes of o -Ps, was followed by a slow crosslinking, given by slight changes in the lifetime of o -Ps.

On the other hand, in Fig. 2b), the courses of τ_{o-Ps} for a series of samples without PI showed the postpone crosslinking stage and post-curing stage for which the one exponential function displayed the best fit. In Table 3, the time constants of the crosslinking stage confirmed that the samples with PI exhibit faster reactions compared to the samples without PI. In addition, for both groups of materials with and without PI, a large amount of VDM showed a slowing of the reactions.

It is worthwhile to explain the connection between time and light energy from Fig. 2(a) and (b). This is explained in the SI.

Fig. 2 The course of photopolymerization for the samples with (a) and without (b) the photoinitiator (PI) investigated via o -Ps lifetime. Two x scales, total irradiation time as “Time” (top X-axis) and light energy absorbed in the sample volume as “Light energy” (bottom X-axis), are displayed

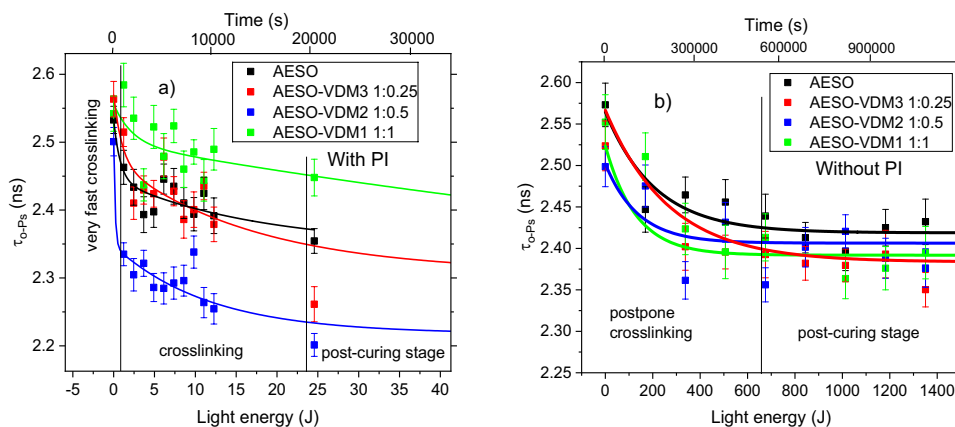


Table 3 Time constants of the exponential fit for biopolymer samples without and with photoinitiator ($y = A_1 \cdot \exp(-x/t_1) + A_2 \cdot \exp(-x/t_2) + y_0$)

with PI	AESO	AESO-VDM3 1:0.25	AESO-VDM2 1:0.5	AESO-VDM1 1:1
t_1 [10^3 s]	0.6	0.8	0.1	1.7
t_2 [10^4 s]	1.3	1.3	0.9	9.5
without PI	AESO	AESO-VDM3 1:0.25	AESO-VDM2 1:0.5	AESO-VDM1 1:1
t_1 [10^3 s]	5.4	3.5	3.3	6.8

Moreover, it is important to take into account that the polymerization runs in the relatively thick samples, in which light absorption also plays a role, specifically for these samples. Therefore, the reduced light intensity is in the volume of the sample at the side of the positron source. As an example, it can be stated that the radiant flux measured at the entrance quartz window was 1.056 mW for a liquid sample and after curing of the 3 mm thick sample was 5.5 μ W, at the sample outlet. The implications of this absorption on network quality will be discussed further in the section on cured samples. At this point, however, we can say that the geometry of the measurement shows that positrons penetrated into the sample in the region of the sample facing away from the light are characterized by slower changes in the local free volumes compared to thermocouples, due to the lower intensity of the light. Therefore, the characteristic response times monitored by PALS are significantly longer than those of thermocouple measurements. This means that the lifetime of *o*-Ps is strongly influenced by the slow polymerization processes just on the sample side at the positron source due to the low intensity of light.

Thus, these time dependences of lifetime changes are an interesting manifestation of the intrinsic shrinkage of the local free volumes and reflect the inhomogeneity of the time course of the reaction in the bulk of the coarse samples.

Characterization of Cross-Linked Samples

NIR Spectroscopy

The series of samples, from PALS experiments, was measured in the middle of cured discs. The intensity of the absorption band at 6172 cm^{-1} reflects the degree of double bond conversion, i.e. consumption of monomers (AESO, VDM), during the photopolymerization. In Fig. 3, an increased amount of VDM in AESO-based cured samples without and with PI showed reduced monomer conversion (AESO, VDM). Lower conversion of double bonds suggests lower cross-linked structure which supports in situ study of photo-networking of AESO-VDM samples without PI by

real-time photorheometry [16] where an increased amount of VDM decreases the value of storage modulus (G') indicating the lower crosslinking density. In the case of the unstudied AESO-VDM samples containing PI by real-time photorheometry, the comparable trend can only be assumed.

Moreover, the cured samples with PI (Fig. 3a) exhibited higher conversion compared to the samples without PI (Fig. 3b). In both cases of biopolymer AESO-VDM samples with and without PI, the increasing amount of VDM leads to the lower conversion of double bonds. However, we are not able to distinguish the acrylate and methacrylate double bonds by NIR.

This finding of decreased conversion of the double bond groups with increasing amount of crosslinking agent VDM may be ascribed to different reactivity of the acrylate and methacrylate double bonds and faster diffusion of VDM than AESO which may cause the formation of local inhomogeneities during networking. To look deeper into the mechanisms of AESO-VDM network formation requires further investigation.

PALS

Figure 4 shows the measured ortho-positronium lifetimes in the samples and their dependence on vanillin dimethacrylate concentration c_{VDM} for sets of cured samples with and without a photoinitiator. In Fig. 4, the samples with a photoinitiator showed shorter lifetimes (by approximately 0.1 ns) compared to samples without a photoinitiator.

More reduced $\tau_{o\text{-Ps}}$ of the samples with and without PI correlates with lower conversion, registered via NIR spectra (Fig. 2a, b). Also, large $\tau_{o\text{-Ps}}$ of all samples without PI correlates with the lower conversion of monomers. These findings from both techniques, NIR and PALS, are important for the possible explanation of the internal structure of investigated biopolymers but they still require further studies of network formation. The reduction of $\tau_{o\text{-Ps}}$ with an increase in the amount of VDM may be due to the aromatic rings which increases the packing efficiency of the cross-linked structure due to stacking π - π interactions and does not necessarily

Fig. 3 NIR spectra of biopolymer samples: with photoinitiator (a) and without photoinitiator (b)

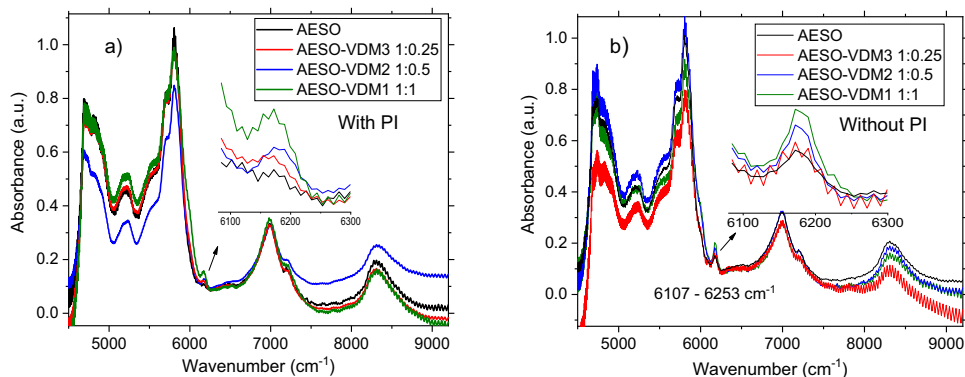
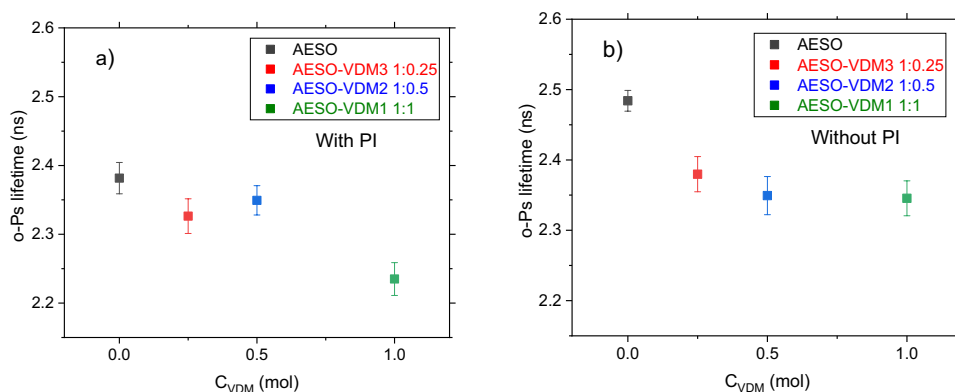


Fig. 4 *o*-Ps lifetime vs. the amount of VDM for a series of cured biopolymer samples with photoinitiator (a) and without photoinitiator (b)



mean a higher crosslink density. However, in the case of the samples without PI, in addition to this main effect of the aromatic VDM rings on the local free volume, there is also the reduced conversion of co-monomers recorded by NIR, which results in a generally larger free volume in comparison with samples with PI.

Table 4 shows the initial lifetime value τ_0 of the monomer mixture, τ_f the final *o*-Ps lifetime after crosslinking and v_{hf} is the corresponding value of the approximate spherical cavity according to relation (2). Evaluation of data was done without dispersion.

Evaluations of the time spectra were also made considering the dispersion of the lifetimes of the *o*-Ps. Since there is a direct interconnection between the *o*-Ps lifetime of the cavity size, e.g. via the TE model, the distribution of lifetimes can be interpreted as a manifestation of the size distribution of the cavities in the material under study. The extraction of dispersion from lifetime spectra is associated with certain complications related to the need for a higher number of pulses in the spectrum under evaluation, its temporal stability of measurements, the choice of an appropriate evaluation program, etc. The LT program allows to determine the dispersion of the lifetime distribution of the selected component and the type of the

distribution is default, it is a lognormal distribution [23]. This implies some predetermined constraints and subjective influences on the resulting distribution of free-volume cavity sizes. Despite these limitations, however, it is at least possible to estimate the basic relative differences between the samples regarding the homogeneity of the crosslinking in terms of the formed free-volume cavities. Thus, given the complexity of the approach, the absolute values of the obtained dispersions will not be discussed further but only the basic trends between samples (relational comparisons) will be compared concerning the VDM concentration and the presence of PI.

The homogeneity of the cross-linked material was characterized using the dispersion of *o*-Ps lifetime distribution (Fig. 5). The dispersion indicates only small difference in the homogeneity of the crosslinking due to the influence of the composition and the presence of the photoinitiator as well as the intensity of the illumination on the final state of the network. It can be concluded that the presence of the photoinitiator and also the lower concentrations of VDM (up to 1:0.5) causes a hint of the reduction of the cavity sizes dispersion. For higher concentrations of VDM (1:1), there is the re-growth in the inhomogeneity of the structure. This trend is also repeated in the samples with PI, where there

Table 4 Characteristic *o*-Ps lifetimes for the liquid state (τ_0) and final cured sample (τ_f) as well as their calculated values of local free volume (v_{hf}) according to Eq. (2) for the samples with and without photoinitiator

Samples with PI	τ_0 [ns]	τ_f [ns]	v_{hf} [nm ³]
AESO	2.53 ± 0.02	2.38 ± 0.02	0.133 ± 0.002
AESO-VDM3 1:0.25	2.56 ± 0.03	2.32 ± 0.03	0.127 ± 0.003
AESO-VDM2 1:0.5	2.50 ± 0.02	2.35 ± 0.02	0.130 ± 0.002
AESO-VDM1 1:1	2.54 ± 0.03	2.23 ± 0.02	0.118 ± 0.002
Samples without PI	τ_0 [ns]	τ_f [ns]	v_{hf} [nm ³]
AESO	2.57 ± 0.03	2.48 ± 0.01	0.144 ± 0.001
AESO-VDM3 1:0.25	2.52 ± 0.03	2.37 ± 0.03	0.133 ± 0.003
AESO-VDM2 1:0.5	2.50 ± 0.03	2.35 ± 0.03	0.131 ± 0.003
AESO-VDM1 1:1	2.55 ± 0.03	2.35 ± 0.02	0.131 ± 0.003

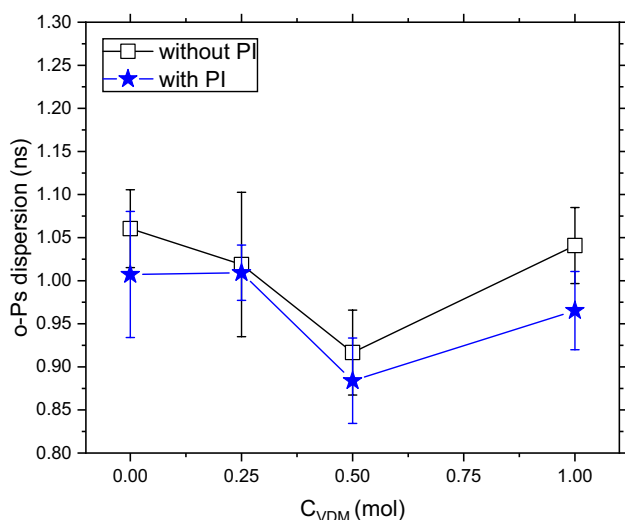


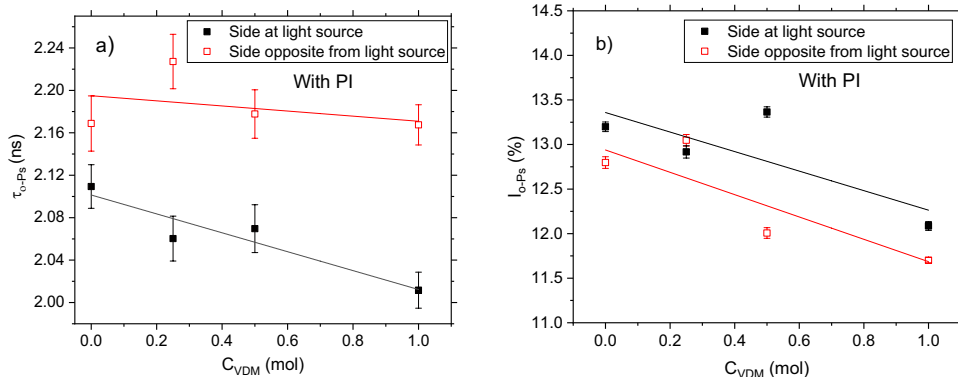
Fig. 5 Dispersion of *o*-Ps lifetime for the samples with and without photoinitiator

is an indication of higher sample homogeneity (narrower dispersion).

This finding of the increased heterogeneity in the samples without PI is in correlation with lower conversion of double bonds obtained in NIR spectra.

The observation of repeated dispersion minima in Fig. 5 for both groups of samples, with and without PI, for VDM concentration about 1:0.5 somewhat complicates ideas about the properties of the samples and the effect of VDM concentration on the free-volume structure. Although this is a minor effect, it is worth noting in further studies of these systems. It is possible that at higher VDM concentrations (1:1) the effect of a higher amount of unreacted double bonds in the AESO-VDM copolymer measured by NIR spectroscopy may be ascribed to the phase separation. Thus, the phase separation could be the reason of increased heterogeneity of the structure. This will be the subject of further studies.

Fig. 6 The VDM concentration dependence of the lifetime of *o*-Ps (a) and intensity of *o*-Ps (b) for continuously illuminated samples with PI obtained from thermocouple measurements



Effect of Sample Thickness on the *o*-Ps Lifetime and the Formation of Ps

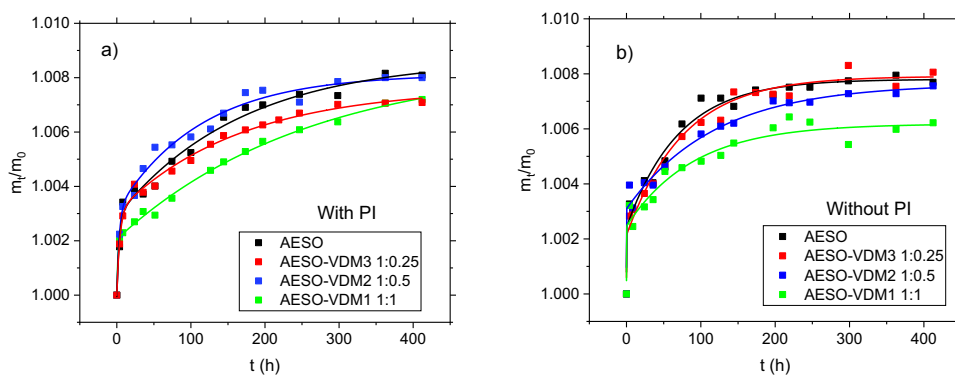
In our series of samples, it was found that a sample thickness of 3 mm already affects networking. The intensity of UV radiation in the material on the side away from the light is lower compared to the side at the light source which is the standard side tested with positrons in our in-situ experiments. In Fig. 6, the cavities are larger (τ_{o-Ps}) and the concentration of cavities (I_{o-Ps}) for the side away from the light is lower than on the side of the sample close to the light source. This finding confirms less crosslinked structure from the side away from the light source. Furthermore, this different light intensity along the sample thicknesses also affects the reaction rate (SI, Fig. S6), which may be a likely source of increased network inhomogeneity. These findings could be related to the three or two stages of crosslinking (fast crosslinking, i.e. acceleration, networking, post-curing) of samples with PI in time (approximated by fast and slow components in Fig. 1a) and by increasing dispersion.

Illustrative linear fits for the lifetimes indicate that with increasing VDM concentration, the effect of structure inhomogeneity between the investigated sides of the sample increases. This heterogeneity of the structure in the volume of the sample also affects the dispersion of the void size expressed through the dispersion of lifetimes, which is large for the highest concentration of VDM. This could be the subject of further investigation.

Sorption and Desorption of Water in the Cured Samples

The process of water diffusion into and out of the samples was investigated from two perspectives. In the first approach, the initial and final state was examined from the point of view of the amount of water that was absorbed in the network of the investigated materials, i.e. standard swelling using water. The dependence of the swelling parameter on the composition of the sample was investigated. The second

Fig. 7 Time dependence of reduced weight m_t/m_0 for swollen samples with photoinitiator (a) and without photoinitiator (b). Solid lines correspond to a 2-exponential fit



approach included also taking into account the time dependence of water sorption and desorption expressed through the time change of the weight of the samples. The purpose of this approach was to estimate the diffusion coefficient of the investigated materials.

The diffusion properties of materials are directly dependent on the free volume properties of the network. The interconnection between the cavities allows the transport of substances into and out of the material. Investigation of the diffusion properties of water in the studied matrices will allow to extend the comprehensive knowledge of the properties of AESO-VDM biopolymers, in aqueous environments, since one of their applications is also as retention matrices for enzymes in biosensors that operate in aqueous environments [7, 8].

Figure 7 shows the time course of water sorption for all samples, with and without a photoinitiator. The parameter m_t/m_0 represents the increase in weight of the samples compared to their original weight, where m_t is the weight of the sample at time t (the weight of the swollen sample) and m_0 is the weight of the original sample (i.e. the sample before swelling, without water).

The S parameters, commonly used to characterize the swelling ability of a polymer in a given solvent, are given in Table 5. S is defined as:

$$S = 100(M_{\text{swollen}} - M_{\text{dry}})/M_{\text{dry}} \quad (3)$$

(in %), where M_{swollen} is the maximal weight of the sample saturated in solvent and M_{dry} is its weight after drying. In our case, we put $m_0 = M_{\text{dry}}$.

In Fig. 8, with the increasing concentration of VDM in the samples, the maximum water sorption decreases. Table 5 shows the reduction in swelling ability, where the S parameter ranges from 0.60 to 0.88. The explanation can be made, for example, that with the increasing proportion of VDM, linear or branched regions are formed in the cross-linked structure, which is more resistant to absorbing water than the cross-linked structure. This was observed in the study of cross- and linear-linked

poly(N-isopropylacrylamide) (PNIPAM) in aqueous solutions where cross-linked networks exhibited much larger water absorption than single-chain swelling [28].

On the other hand, we can also consider the effect of a reduced local free volume of cured sample with an increase in the concentration of VDM, which reduces the local free volumes of the network, slow down diffusion into the volume, and reduce the ability to sorb water into the sample volume.

The second approach to the investigation of sorption and desorption of water in the samples with different content of VDM and photoinitiator was to investigate the time dependence of the weight of water in the samples in order to estimate the diffusion coefficient for water in cross-linked polymers. The diffusion coefficient (D) is a constant that characterizes how easily a substance can diffuse into the environment. It depends on the temperature, the viscosity and the size of the diffusing particles [29]. In our case, the diffusion coefficients for individual samples were determined by a procedure that is briefly explained in the following paragraph and described in more detail in the work [8] in appendix S1. The dependence of the measured sample mass m on time t was used to evaluate the diffusion constant of water molecules absorbed in the sample (D) using the concept of the mean first transit time τ . In the desorption process, a particle is present in the sample at time $t=0$ and then diffuses until it hits the boundary and evaporates. The probability of survival of a particle in the sample at time t is $P(t)$. Then τ is defined as:

$$\tau = \int_0^{\infty} t \left(-\frac{dP(t)}{dt} \right) dt = \int_0^{\infty} P(t) dt \quad (4)$$

We further assume that $P(0)=1$ represents the probability that the particle is definitely in the system. $P(t \rightarrow \infty)=0$ represents the probability that the particle is certainly not present in the system and $-dP(t)/dt$ represents the probability density, that the particle leaves the sample at time t . In the one-particle approximation, we consider that water molecules do not limit each other. Thus, the mass of the

Table 5 The swollen characteristics of the investigated polymer samples with and without photoinitiator. Swellability of a series of investigated samples with and without PI

Samples with PI	$M(t)_{\max}/M_0$ (g/g), swell	$S, \%$
AESO	1.00809	0.809
AESO-VDM3 1:0.25	1.00708	0.875
AESO-VDM2 1:0.5	1.008	0.706
AESO-VDM1 1:1	1.00702	0.720
Samples without PI	$M(t)_{\max}/M_0$ (g/g), swell	$S, \%$
AESO	1.00769	0.795
AESO-VDM3 1:0.25	1.00806	0.755
AESO-VDM2 1:0.5	1.00756	0.728
AESO-VDM1 1:1	1.00622	0.598

sample m_t at time t depends linearly on the survival probability $P(t)$, which we can write as:

$$P(t) = \frac{(m_t - m_\infty)}{(m_0 - m_\infty)} \quad (5)$$

where m_0 and m_∞ represent the initial and final values for desorption (wet and dry samples). The numerical integration of the obtained $P(t)$ is τ , which can be used to estimate the diffusion coefficient D of water in the investigated substances at laboratory temperature (20 °C) [28]:

$$D = \frac{d^2}{12\tau} \quad (6)$$

where d is the thickness of the sample. The relation applies to thin cylindrical samples with a radius $R \gg d$, which is satisfied in our case. The water absorption can be described by a similar process in which the vacancies diffuse from the sample. Then we arrive at the survival probability:

$$P(t) = \frac{(m_{\max} - m_t)}{(m_{\max} - m_{\min})}, \quad (7)$$

where m_{\min} , m_{\max} denote minimum and maximum mass of the sample at the beginning of the swelling and of the saturated state, respectively. The diffusivity of the water molecules and of their vacancies is the same in the single particle approximation, so we obtain it again from Eq. (6).

Figure 9 represents normalized water sorption curves $P(t)$ according to Eq. (7). The mean first transit time τ integrated numerically from these curves gives in the diffusion coefficient according to relation (6). The results for the samples with or without PI depending on the VDM concentrations are shown in Fig. 10. It can be concluded that the magnitude of the diffusion coefficient for water has

a decreasing trend with an increase in the concentration of VDM and also decreases with the presence of PI.

The values of the D coefficients obtained for desorption, calculated from the curves, according to formula (5) are of similar order and are presented in the SI together with further auxiliary data (Table S1, S2, Fig. S3–S5).

The deviations of D determined during desorption from the values obtained from sorption are because the boundary conditions of both experiments were not completely identical. Desorption took place spontaneously in the air with non-zero air humidity, so the curves converged to a higher final weight value. On the other hand, the initial value of the weight of the matrix and absorbed water during the desorption process was burdened by a possible deficit of the weight of the matrix due to the leaching of unreacted parts out of the matrix during swelling.

Conclusions

In-situ reaction courses were measured during intermittent illumination by the PALS technique for biopolymer AESO-VDM samples with different concentrations of VDM and with or without PI. It was found that the samples with the addition of a photoinitiator reduced the local free volume significantly faster than the samples without PI and the samples with the increasing concentration of VDM decelerate crosslinking. In order to clarify the course of the reaction in the initial stages, the course of the reaction was also measured during continuous illumination using thermocouples (TC) in the same geometry of the samples as in the PALS measurements. It was revealed that increasing amount of VDM in AESO-based samples with or without PI accelerates the reaction at the beginning which also reflects more or less phase separation via t_{JP} . But increasing values of t_{\max} in a series of AESO-VMD samples with or without PI

Fig. 8 The VDM concentration dependence of S parameter for samples with photoinitiator (a) and without photoinitiator (b)

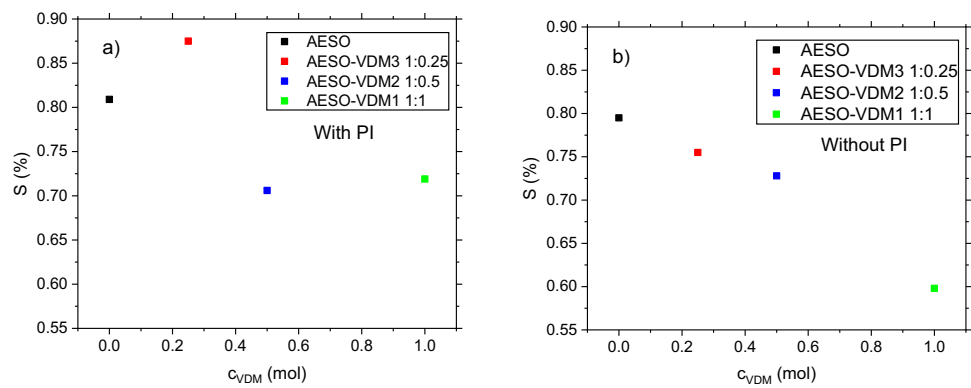


Fig. 9 Time dependence of mass ratio $(m_{max}-m_t)/(m_{max}-m_{min})$ for samples with photoinitiator (a) and without photoinitiator (b) at the process of sorption

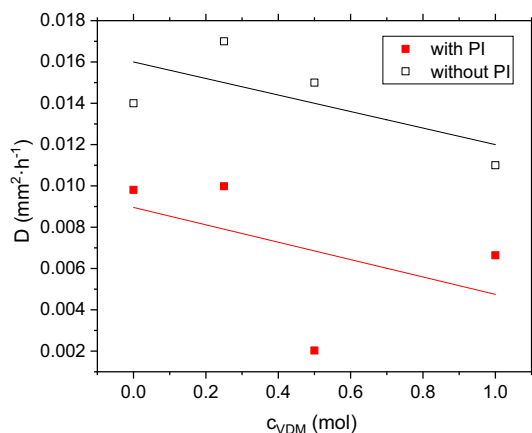
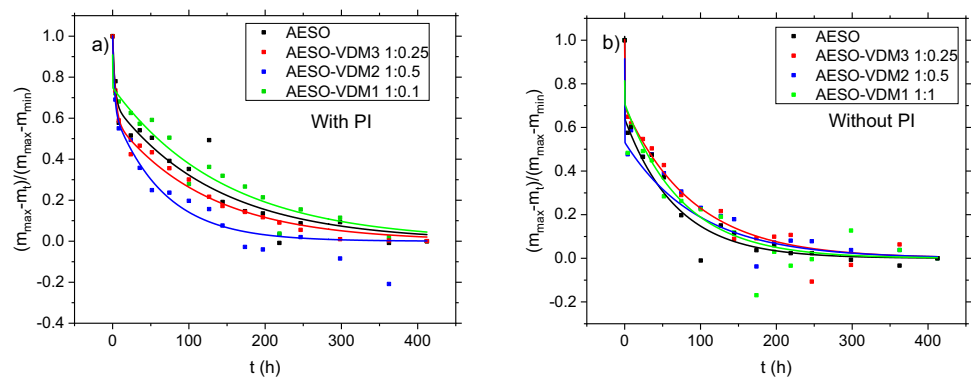


Fig. 10 The magnitude of the diffusion coefficient calculated via sorption as a function of the VDM concentration

confirmed that higher amount of VDM causes slowing down of reaction.

Both, TC and PALS time measurements showed the slowest course of reaction for the highest concentration of VDM in the AESO-VDM sample.

Next, the free volume characteristics (PALS), the conversion of double bonds (NIR) and experiments with water sorption and desorption with the evaluation of the diffusion

coefficient for the final cured AESO-based samples with or without PI were mutual compared.

PALS

As the concentration of vanillin dimethacrylate increased, the size of the free volumes in all samples in the cross-linked state decreased from 0.133 to 0.118 nm³ with a photoinitiator and from 0.144 to 0.131 nm³ without a photoinitiator.

Samples with the addition of a photoinitiator showed smaller sizes of free volumes in the cross-linked state compared to samples without the addition of a photoinitiator, which implies that the photoinitiator has an effect not only on the speed of the photopolymerization itself but also on the final microstructural properties of the hardened material.

PALS measurements showed different cross-linking homogeneity on the side of the sample near the light source and on the opposite side, for 3 mm thick samples with PI.

This finding is a consequence of different absorption of light in the investigated materials. Absorption of UV light in these samples causes different light intensities in the area of the ongoing reaction and thus different cross-linking speeds. This was manifested mainly in samples with PI due to the biphasic nature of the course in the decrease in the lifetime of *o*-Ps. On the side of higher light intensity, the holes are smaller and there are probably more of them, as indicated

by the higher value of the intensity of *o*-Ps formation. As the concentration of VDM increased, the effect of inhomogeneity of the structure between the examined sides of the samples increased.

NIR Spectroscopy

Showed that increasing concentration of VDM causes lowering conversion of C=C double bonds for both types of biopolymer samples, with and without PI. Moreover, biopolymer samples with PI were more cross-linked, indicating higher conversion of C=C double bonds. From this point of view, pure AESO + PI should have the highest conversion of double bonds and thus the maximum crosslinking.

Sorption and Desorption of Water

It was found that an increased concentration of VDM in the samples, slowing down the water sorption process which correlates with the formation of reduced local free volumes in the network (PALS). The *S* parameter determined from the sorption curve (initial and final weight value) generally decreased with increasing VDM concentration. Probably, the presence of aromatic rings in parts of the network from VDM reduced the local free volumes in the network, which prevented water sorption more in the samples with a rich representation of VDM compared to pure AESO. Such an explanation is more realistic than the idea that the low swellability (small *S* parameter) is caused by a high crosslink density, which in our case would be inconsistent with the NIR finding.

The water diffusion coefficients for the investigated samples were determined from the sorption and desorption curves. Here, the magnitude of the diffusion coefficient has a decreasing trend with the increased concentration of VDM, which is in accordance with the above mentioned findings.

It can be concluded that VDM admixtures as well as the presence of a photoinitiator affect (reduce) the size of free-volume cavities, the quality of crosslinking (crosslink density) and diffusion properties, which were tested on water.

The control of these parameters opens a possibility to adapt the biopolymers to be an optimal matrix for the immobilization of different in-size biomolecules (large or very small).

In summary, by using different amounts of vanillin dimethacrylate and with or without a photoinitiator it is possible to vary the local free volume and diffusion properties in the AESO-VDM biopolymers which are used as enzyme-immobilizing matrix.

Supplementary Information The online version contains supplementary material available at <https://doi.org/10.1007/s10924-023-03097-1>.

Acknowledgements The authors thank the Slovak Research and Development Agency (project No. APVV-21-0335) and Slovak Grant Agency VEGA (projects Nos. 2/0137/23 and 2/0161/20) for the support of research finding. This study was also supported by the Operation Program of Integrated Infrastructure for the project, UpScale of Comenius University Capacities and Competence in Research, Development and Innovation, ITMS2014+: 313021BUZ3, co-financed by the European Regional Development Fund, the Ministry of Education and Science of Ukraine (projects Nos. 0121U109543, 0122U000850, 0122U000874, and 0123U103572), and National Research Foundation of Ukraine (projects Nos. 2020.02/0100 “Development of new nanozymes as catalytic elements for enzymatic kits and chemo/biosensors” and 2021.01/0010 “Development of an enzymatic kit and portable biosensors for express-analysis of creatinine, a marker of acute functional disorders of the kidneys”). D.P.K. also thanks the Comenius University youth grant (project No. UK/53/2022). T.K. also acknowledges the SAIA (Slovak Academic Information Agency) for scholarship in the Institute of Physics of Slovak Academy of Sciences in the framework of the National Scholarship Programme of the Slovak Republic. This work has also received funding through the MSCA4Ukraine project (Grant No. 1128327), which is funded by the European Union.

Author Contributions Conceptualization (HŠ, OŠ), Data curation (OŠ, PK, HŠ), Formal analysis (DPK, HŠ, KC, OŠ), Funding acquisition (HŠ, TK), Investigation (DPK, KC, HŠ, DT, OŠ, PK, TK, JO, OS, MG, VS, AK), Methodology (HŠ, OŠ, TK), Project administration (HŠ, OŠ, TK), Resources (HŠ, OŠ, TK, JO), Supervision (HŠ, TK), Writing—original draft (HŠ, OŠ, TK), Writing—review & editing (DPK, KC, HŠ, OŠ, PK, TK, JO, OS, MG, VS, AK).

Funding Open access funding provided by The Ministry of Education, Science, Research and Sport of the Slovak Republic in cooperation with Centre for Scientific and Technical Information of the Slovak Republic. Comenius University youth grant, project No. UK/53/2022, Vedecká Grantová Agentúra MŠVVaŠ SR a SAV, project No. 2/0137/23 and 2/0161/20 the Operation Program of Integrated Infrastructure for the project, UpScale of Comenius University Capacities and Competence in Research, Development and Innovation, ITMS2014 + : 313021BUZ3, Agentúra na Podporu Výskumu a Vývoja, project No. APVV-21-0335, European Regional Development Fund, the Ministry of Education and Science of Ukraine, Nos. 0121U109543, 0122U000850, 0122U000874, and 0123U103572, Slovak Academic Information Agency, National Research Foundation of Ukraine, projects Nos. 2020.02/0100 and 2021.01/0010, MSCA4Ukraine, Grant No. 1128327.

Declarations

Competing interest The authors declare no competing interests.

Open Access This article is licensed under a Creative Commons Attribution 4.0 International License, which permits use, sharing, adaptation, distribution and reproduction in any medium or format, as long as you give appropriate credit to the original author(s) and the source, provide a link to the Creative Commons licence, and indicate if changes were made. The images or other third party material in this article are included in the article's Creative Commons licence, unless indicated otherwise in a credit line to the material. If material is not included in the article's Creative Commons licence and your intended use is not permitted by statutory regulation or exceeds the permitted use, you will need to obtain permission directly from the copyright holder. To view a copy of this licence, visit <http://creativecommons.org/licenses/by/4.0/>.

References

- Sagermano M (2012) Advances in cationic photopolymerization. *Pure Appl Chem* 84:2089–2101. <https://doi.org/10.1351/PAC-CON-12-04-11>
- Yagci Y, Jockusch S, Turro N (2010) Photoinitiated polymerization: advances, challenges, and opportunities. *Macromolecules* 43:6245–6260. <https://doi.org/10.1021/ma1007545>
- Fouassier JP (1995) Photoinitiation, Photopolymerization, and photocuring: fundamentals and applications. Hanser/Gardner Publications, Munich
- Kloosterboer JG, Network formation by chain crosslinking photopolymerization and its applications in electronics. In: *Electronic Applications. Advances in Polymer Science*, Vol. 84, Springer-Verlag, Berlin, Heidelberg, 1988.
- Kavetsky T, Smutok O, Demkiv O, Kasetaitė S, Ostrauskaite J, Švajdlenková H, Šauša O, Zubrytska K, Hoivanovych N, Gonchar M (2019) Dependence of operational parameters of laccase-based biosensors on structure of photocross-linked polymers as holding matrixes. *Eur Polym J* 115:391–398. <https://doi.org/10.1016/j.eurpolymj.2019.03.056>
- Kavetsky T, Yuliia K, Zubrytska K, Khalilov R, Smutok O, Demkiv O, Šauša O, Švajdlenková H, Gonchar M (2019) Construction of amperometric laccase-based biosensors using the ureasil and photocross-linked polymers. *Adv Biol Earth Sci* 4:137–149
- Gozdziuk M, Zgardzinska B, Kavetsky T, Zubrytska K, Smutok O, Šauša O, Lebedevaite M, Ostrauskaite J, Kiv A (2021) Nanostructure research and amperometric testing to determine the detection capabilities of biopolymer matrices based on acrylated epoxidized soybean oil. *Acta Phys Pol A* 139:432–437. <https://doi.org/10.12693/APhysPolA.139.432>
- Godziuk M, Kavetsky T, Roquero DM, Smutok O, Gonchar M, Kráľovič DP, Švajdlenková H, Šauša O, Kalinay P, Nosrati H, Lebedevaite M, Grauzeliene S, Ostrauskaite J, Kiv A, Zgardzińska B (2022) UV-cured green polymers for biosensors: correlation of operational parameters of highly sensitive biosensors with nano-volumes and adsorption properties. *Materials* 15:6607. <https://doi.org/10.3390/ma15196607>
- Petric RA (1997) Positron annihilation—a probe for nanoscale voids and free volume? *Prog Polym Sci* 22:1–47. [https://doi.org/10.1016/S0079-6700\(96\)00023-8](https://doi.org/10.1016/S0079-6700(96)00023-8)
- Schrader DM, Jean YC (eds) (1988) *Positron and Positronium Chemistry*. Elsevier, Amsterdam
- Goworek T (2014) Positronium as a probe of small free volumes in crystals, polymers and porous media. *Ann. Univ. Mariae Curie-Skłodowska, Lublin—Polonia* 69:1–10. <https://doi.org/10.2478/umcschem-2013-0012>
- Švajdlenková H, Šauša O, Peer G, Gorsche C (2018) In situ investigation of the kinetics and microstructure during photopolymerization by positron annihilation technique and NIR-rheology. *RSC Adv* 8:37085–43709. <https://doi.org/10.1039/C8RA07578F>
- Ferrell RA (1957) Long lifetime of positronium in liquid helium. *Phys Rev* 108:167–168. <https://doi.org/10.1103/PhysRev.108.167>
- Stewart AT, Roelig LO, Eds., *Positron Annihilation*, Academic Press, New York, 1967, p. 127.
- Buchikhin AP, Goldanski VI, Shantarovich VP (1971) Temperature dependence of the lifetime of triplet positronium in aliphatic hydro-carbons and their derivatives. *Pis'ma Zh. Exp Teor Fiz* 13:624.
- Lebedevaite M, Ostrauskaite J, Skliutas E, Malinauskas M (2019) Photoinitiator free resins composed of plant-derived monomers for the optical μ -3D printing of thermosets. *Polymers* 11:116. <https://doi.org/10.3390/polym11010116>
- Remeikyte A, Ostrauskaite J, Grazuleviciene V (2013) Synthesis and properties of photocross-linked polymers of epoxidized linseed oil with different reactive diluents. *J Appl Polym Sci* 129:1290–1298. <https://doi.org/10.1002/app.38816>
- Kasetaitė S, Ostrauskaite J, Grazuleviciene V, Svediene J, Bridziuviene D (2014) Camelina oil- and linseed oil-based polymers with bisphosphonate crosslinks. *J Appl Polym Sci* 131:40683. <https://doi.org/10.1002/app.40683>
- Kasetaitė S, Ostrauskaite J, Grazuleviciene V, Svediene J, Bridziuviene D (2015) Photocross-linking of glycerol diglycidyl ether with reactive diluents. *Polym Bull* 72:3191–3208. <https://doi.org/10.1007/s00289-015-1461-x>
- Lebedevaite M, Ostrauskaite J (2021) Influence of photoinitiator and temperature on photocross-linking kinetics of acrylated epoxidized soybean oil and properties of the resulting polymers. *Ind Crops Prod* 161:113210. <https://doi.org/10.1016/j.indcrop.2020.113210>
- Petriska M, Sojak S, Slugeň V (2014) Positron lifetime setup based on DRS4 evaluation board. *J Phys Conf Ser* 505:012044. <https://doi.org/10.1088/1742-6596/505/1/012044>
- Petriska M, Sojak S, Kršjak V, Slugeň V (2021) Digital triple coincidence positron lifetime setup with DRS4 and its benefits. *AIP Conf Proc* 2411:080009. <https://doi.org/10.1063/5.0067492>
- Kansy J (1996) Microcomputer program for analysis of positron annihilation lifetime spectra. *Nucl Instrum Methods Phys Res Sect A* 374:235–244. [https://doi.org/10.1016/0168-9002\(96\)00075-7](https://doi.org/10.1016/0168-9002(96)00075-7)
- Tao SJ (1972) Positronium annihilation in molecular substances. *J Chem Phys* 56:5499–5510. <https://doi.org/10.1063/1.1677067>
- Eldrup M, Lightbody D, Sherwood JN (1981) The temperature dependence of positron lifetimes in solid pivalic acid. *Chem Phys* 63:51–58. [https://doi.org/10.1016/0301-0104\(81\)80307-2](https://doi.org/10.1016/0301-0104(81)80307-2)
- Švajdlenková H, Kleinová A, Šauša O, Rusnák J, Dung TA, Koch T, Knaack P (2020) Microstructural study of epoxy-based thermosets prepared by “classical” and cationic frontal polymerization. *RSC Adv* 10:41098–41109. <https://doi.org/10.1039/D0RA08298H>
- Jagtap A, More A (2022) A review on self-initiated and photoinitiator-free system for photopolymerization. *Polym Bull* 79:8057–8091. <https://doi.org/10.1007/s00289-021-03887-4>
- Lopez CG, Scotti A, Brugnoli M, Richtering W (2018) The Swelling of poly(Isopropylacrylamide) near the θ temperature: a comparison between linear and cross-linked chains. *Macromol Chem Phys* 220:1800421. <https://doi.org/10.1002/macp.20180421>
- Haun W, Coffmann A, Clasen B (2014) Improved soybean oil quality by targeted mutagenesis of the fatty acid desaturase 2 gene family. *Plant Biotechnol J* 12:934–940. <https://doi.org/10.1111/pbi.12201>

Publisher's Note Springer Nature remains neutral with regard to jurisdictional claims in published maps and institutional affiliations.